Open Archive Toulouse Archive Ouverte (OATAO)

OATAO is an open access repository that collects the work of Toulouse researchers and makes it freely available over the web where possible.

Any correspondence concerning this service should be sent to the repository administrator: staff-oatao@listes.diff.inp-toulouse.fr

Electrochemical Kinetic Study of LiFePO$_4$ Using Cavity Microelectrode

J. Come,[a] P.-L. Taberna,[a] S. Hamelet,[b] C. Masquelier,[b] and P. Simon[a,z]

[a]*Université Paul Sabatier, CIRIMAT UMR CNRS 5085, 31062 Toulouse Cedex 4, France*
[b]*Université de Picardie Jules Verne, LRCS, UMR CNRS 6007, 80000 Amiens, France*

Lithium cation insertion and extraction in LiFePO$_4$ were electrochemically studied with a cavity microelectrode (CME). Cyclic voltammetry measurements were used to characterize the kinetics of the material. LiFePO$_4$ was successfully cycled from 0.1 mV s^{-1} up to 1 V s^{-1} and is therefore a suitable material to be used in high power applications, such as asymmetric hybrid supercapacitors. Several kinetic behaviors were observed depending on the sweep rate. The LiFePO$_4$ was found to follow different kinetics behaviors depending of the sweep rate. The charge storage mechanisms were investigated for Li$^+$ extraction/insertion.

Lithium iron phosphate LiFePO$_4$ (LFP) has been extensively studied as a promising cathode material for lithium-ion batteries as it possesses several advantages over other cathode materials such as abundance and low cost of raw materials, improved safety performance and a theoretical capacity of 170 mAh/g.[1] Lithium insertion/extraction occurs at a flat 3.42 V vs Li$^+$/Li voltage plateau in a two-phase reaction FePO$_4$/LiFePO$_4$ during galvanostatic discharge.[1,2] However the power performance of the LiFePO$_4$ is limited by its low intrinsic electronic conductivity (ca. 10^{-10} S.cm^{-1})[3] and Li$^+$ diffusivity (ca. 10^{-10}–10^{-16} cm^2 s^{-1}).[4,5] Thus, many efforts have been made to improve the high rate capability including carbon coating and decreasing particle size.[3,6] For example, Kang et al. recently reported a discharge rate as high as 400C thanks to a thin amorphous layer at the surface of the LFP particles that enhanced the charge carrier mobility.[7] Although 65 wt % of carbon conducting additives was used to obtain such a high rate, these results highlight the excellent intrinsic kinetics properties of LiFePO$_4$-based electrodes. Electrochemical double layer capacitors are power devices but suffer of poor energy density. Attempts to increase the specific energy lead undoubtedly to decrease the power performance. Asymmetric hybrid supercapacitors involving a capacitive activated carbon electrode and a faradic Li$^+$ insertion electrode are emerging as a high energy density technology. However, the kinetic properties of the faradic electrode would set the power performances of the asymmetric device.

This work aims at studying the kinetic performances of a slightly non-stoichiometric carbon-coated LiFePO$_4$ at very high insertion/deinsertion rates by cyclic voltammetry. Several studies recently demonstrated that the Li$^+$ insertion/extraction occurs at the phase boundary along the [010] axis, which invalidates the "shrinking-core" model for LiFePO$_4$.[8–16] The Li$^+$ ions diffuse through the particle-electrolyte interface and within the olivine structure in a one dimensional non-linear pathway. The high rate performance measurements of LiFePO$_4$, in contradiction with its low intrinsic electronic conductivity, can be explained by the high mobility of charge carriers (Li$^+$ ions and electrons) at the Li-rich/Li-poor phase boundary. We show here the importance of the active sites located at the surface of the particles for charge storage capability at very high rates.

Experimental

Li$_{0.98}$FePO$_4$ particles with an average diameter of 140 nm were obtained by a straight forward precipitation route as described in reference.[17] A thin layer of conducting carbon coating (2.5 wt %) was then deposited through spray-drying and further annealing at ∼650°C, giving rise to spherical porous agglomerates as seen in Fig. 1. The value of the unit-cell volume (290.5 Å^3) is consistent with slightly oxidized (non-stoichiometric) "LiFePO$_4$".

[z] E-mail: simon@chimie.ups-tlse.fr

Figure 2 shows a schematic of the cavity microelectrode used in this study. It consists in a thin platinum wire (diameter = 60 μm) sealed into a low melting glass onto which a laser beam was focused to dig a cavity of 30 μm in diameter and 40 μm in depth. The platinum wire was connected to a copper wire current collector. A close electrical contact between both wires was ensured by the addition of carbon graphite powder inside the holding glass. A cavity microelectrode presents several advantages compared to conventional electrochemical setup since (i) simple and fast experiments can be carried out and (ii) few microgram of active material are needed which enables very high cycling rates up to several volts per second (the ohmic drop is drastically decreased).

The active material preparation was made by mixing the LFP powder with conductive carbon black additive (TimCal super C65) in a 1:1 weight ratio. The amount of conducting carbon additive is of course irrelevant for the use in a practical device, but it enables to keep a close electrical contact between particles and therefore allows stable and reproducible cycling conditions. Moreover, the carbon black addition allowed us to decrease further the ohmic drop (electronic transport through the matrix) and focus only on the transport properties in the material.[18] The mixture was dried for 24 h at 80°C before any electrochemical characterization had been performed. The dried powder was pressed manually inside the
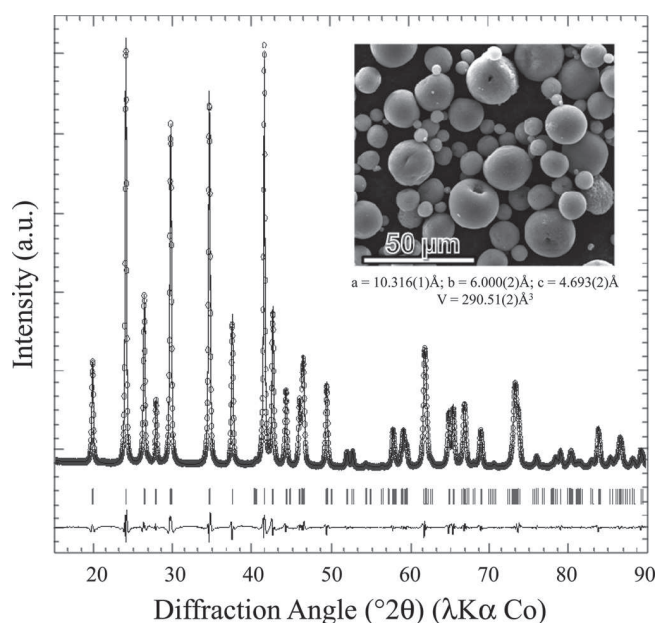

Figure 1. XRD pattern for a carbon-coated LiFePO$_4$ sample. The Inset shows a SEM picture of the LFP agglomerates.
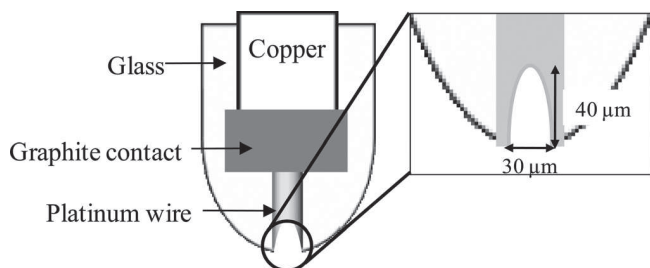
Figure 2. Schematic of the cavity microelectrode.

microcavity and introduced in the measurement cell. A 1 cm² rolled platinum foil was used as the counter electrode and a piece of lithium metal as the reference electrode. The electrochemical cells were assembled in a glove box under Argon atmosphere (5.0) to prevent any moisture contamination. The electrochemical tests were performed at room temperature in 1M $LiPF_6$ dissolved in EC:DMC (1:1). Before any experimental data were recorded, the fresh working electrode was cycled at 20 mV s⁻¹ for 20 times between 4.2 and 2.5 V vs Li⁺/Li to be sure that the steady state was reached, and to remove surface water from the $LiFePO_4$ particles.

Results and Discussion

Figure 3 shows the CV curves of $LiFePO_4$ from 10 mV s⁻¹ up to 1 V s⁻¹. The shape of the curves is kept the same whatever the scan rate and no distortion due to ohmic losses is observed even at 1 V s⁻¹ (corresponding to a time of charge and discharge of ca. 2.5 s). The stability of the CV signal at such rate reveals the high power capability of the LFP and enables kinetic analysis on a broad sweep rate range. Current peaks are observed, corresponding to the oxidation (positive current) and the reduction (negative current) of the material upon cycling standing for the extraction of Li⁺ ions from the LFP and Li⁺ insertion in the delithiated $FePO_4$ phase, respectively.[1,2] Figure 4 shows the peak potentials as a function of the scan rate. The peak separation is 60 mV at 0.1 mV s⁻¹ and increases with the sweep rate with 60 mV per decade until 5 mV s⁻¹, as shown in the inset of Fig. 4. At higher scan rate (>5 mV s⁻¹) the peak separation increases drastically and reaches 300 mV per decade from 500 mV s⁻¹ to 1 V s⁻¹. If the peak separation for a quasi-reversible reaction is 60/αn mV for each tenfold increase in v, the increase of
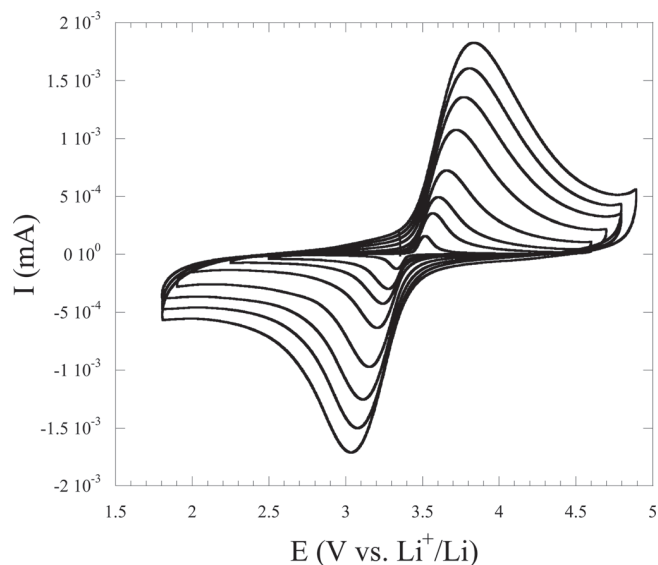

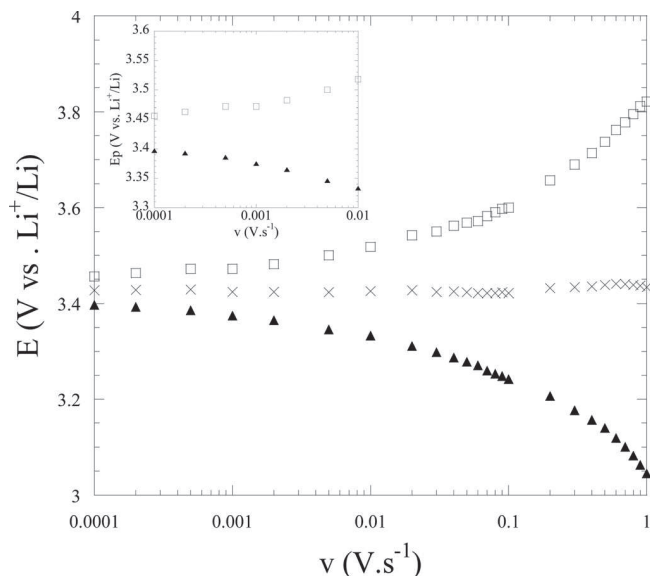**Figure 4.** Anodic (white squares) and cathodic (black triangles) peak potentials, and mean peak potential (Epa + Epc)/2 (crosses) as a function of the scan rate. Inset shows a magnification from 0.1 to 10 mV s⁻¹.

the peak separation is due to the decrease of the αn term, with α the transfer coefficient and n the number of exchanged electrons. The LFP can thus be considered as a quasi-reversible system.[19] Figure 4 shows also that the mean potential, i.e. the average value between anodic and cathodic peaks, is constant at 3.43 V vs Li⁺/Li on the whole range of sweep rates, in accordance with the value reported by Matsui et al.[20] The peak shift magnitude is thus the same for both charge and discharge processes. This, associated with the symmetry of the signal during oxidation and reduction suggests no significant difference of the charge storage mechanism between both reactions up to 1 V s⁻¹.

For a two-phase charge transfer process, like for the $LiFePO_4$/$FePO_4$ system, the Li⁺ extraction/insertion leads to a current peak whose intensity depends on the scan rate following a power law

$$Ip = av^b \tag{1}$$

where Ip is the peak intensity in A, v the scan rate in V s⁻¹, a and b are adjustable coefficients. For a Nernstian (reversible) system, i-e a system for which the rate-limiting step is governed by the mass transport, both anodic and cathodic peak intensities would show the same magnitude. However it is not the case in our study and it has already been demonstrated in a CV study of LFP that the two-phase reaction processes during charge and discharge make the Li⁺ ions diffuse in different electrochemical environments that may account for the peak magnitude.[19] Both observations about peak potential and intensity show that the $LiFePO_4$/$FePO_4$ two-phase system must be considered as electrochemically irreversible in the studied sweep rate range.

Additionally, the power law in Eq. 1 is widely used to determine the rate-limiting step of an electrochemical reaction.[19–23] The b-exponent takes values between 0.5 and 1, whether the reaction is limited by the linear diffusion of the reactive species (b = 0.5) or by the charge transfer (b = 1).[24] Figure 5 shows the change of the peak current versus the potential scan rate in a logarithm scale. Despite a slight change of the slope observed at ca. 10 mV s⁻¹, the average b coefficients calculated from Eq. 1 were found to be 0.53 and 0.55 for the anodic and cathodic processes, respectively. It is not surprising since the Li⁺ insertion/deinsertion process into LFP is known to be diffusion limited.[20,21]

However, this basic representation does not accurately highlight the changes in the kinetic behavior of the system and its

Figure 3. CV curves of carbon-coated $LiFePO_4$ from 10 mV s⁻¹ to 1 V s⁻¹ in LP30 electrolyte obtained with the cavity microelectrode.
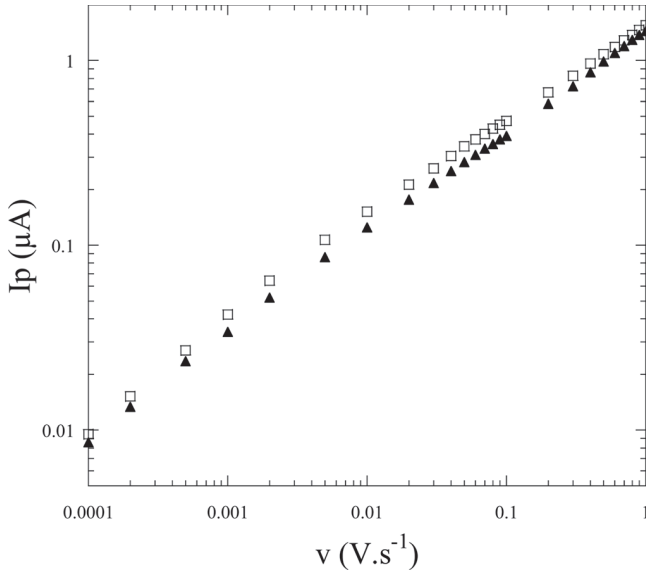
Figure 5. Plot of the anodic (white squares) and cathodic (black triangles) peak intensities as a function of the scan rate in a logarithm scale.

interpretation is often limited to whether the process is diffusion-limited or not without further information on the mechanism of the process.[20–23] A study on the pseudocapacitive electrochemical behavior of TiO_2 nanoparticles showed indeed that the total measured current can be divided into two contributions.[25] One part of the current is considered to change with the scan rate while another part to vary with the square root of the scan rate, as shown in the following Eq. 2

$$Ip = k_1 v + k_2 v^{1/2} \qquad (2)$$

which can be rearranged in

$$Ip/v^{1/2} = k_1 v^{1/2} + k_2 \qquad (3)$$

Two different contributions to the total measured current are thus observed. The non solid diffusion-limited contribution is defined by the k_1 coefficient, associated with a fast surface process, and a diffusion-limited faradic reaction defined by the k_2 coefficient. Consequently, it becomes possible to determine the phenomenon governing the reaction kinetics by calculating the ratio k_1/k_2 and thus to accurately observe the changes in the kinetic behavior of the material. Considering Eq. 3 and plotting $I/v^{1/2}$ versus $v^{1/2}$, k_1 would thus be the slope of the plot, and k_2 its y-intercept. In this respect Fig. 6a shows the anodic and cathodic peak intensities according to Eq. 3 from 0.1 mV.$^{-1}$ to 1 V s^{-1}. It reveals that the charge storage process follows several kinetic behaviors depending on the sweep rate, which can be split into three zones. The k_1 and k_2 coefficients are then listed in Table I.

At low scan rate the k_1 value was much superior to the k_2 coefficient, giving a k_1 coefficient that yields for ca. 90% of the total current for both oxidation and reduction. The high k_1/k_2 ratio means that the increase of the current is proportional to the scan rate instead of its square root. The meaning of such behavior is not that the charge storage takes place in a capacitive way, but that the system is not limited by the Li$^+$ solid diffusion (up to ca. 5 mV s^{-1}) and behaves like a thin-layer: the lithiation/delithiation occurs in the entire bulk of the particles and all the sites for oxidation and reduction participate to the process, allowed by a fast mobility of the Li$^+$ ions within the low-ordered phase boundary region without concentration gradient, as suggested by Chen et al.[8] This is consistent with the plot in Fig. 6b that shows the relative amount of charge stored and released as a function of the scan rate. It can be observed that at
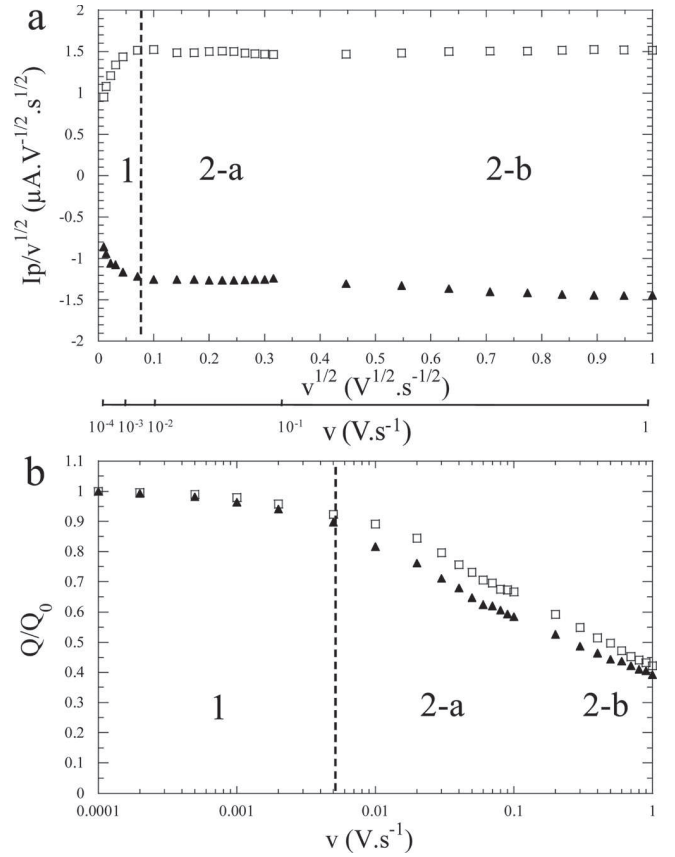

Figure 6. (a) Plot of $Ip/v^{1/2}$ versus $v^{1/2}$ from 0.1 mV s^{-1} to 1 V s^{-1}, a logarithm scale is shown below. (b) Relative charge as a function of the scan rate from 0.1 mV s^{-1} to 1 V s^{-1}. Anodic (white squares) and cathodic (black triangles) reactions are represented. Dotted line is fixed at 5 mV s^{-1} in both plots.

low scan rate the relative amount of charge varies very little with the sweep rate, since still 90% of the capacity is kept at 5 mV s^{-1} as compared to that measured at 0.1 mV s^{-1}. For higher scan rates, the k_1 coefficient (slope) tends to zero. A zero k_1 coefficient means a pure diffusion-limited process. It becomes likely that there exists a critical sweep rate value (in the present case 5 mV s^{-1}) from which the kinetic behavior of LFP is radically different. The solid diffusion of Li$^+$ ions becomes the rate limiting step of the reaction and all the sites for the oxidation and reduction are no longer active. This is illustrated as well in Fig. 6b, as the charge stored decreases sharply from ca. 5 mV s^{-1}. In this region, the kinetic of the reaction is controlled by a concentration gradient.

A closer look at the plots in Fig. 6 yields to consider a third zone (referred to as 2-b) from 100 mV s^{-1} to 1 V s^{-1}. The k_1 contribution to the total current in this region accounts for 5 and 20% respectively for the anodic and cathodic reactions. The increase of the k_1 coefficient and the constant loss of the passed charge with the sweep rate in this range reveal that an increasing part of the current is due to the fast reaction at the surface of the particles, which is not a process limited by the transport of Li$^+$ ions and commonly called pseudocapacitance.[25] The difference in the k_1/k_2 ratio between anodic and cathodic reactions may arise from the faster electron transfer in $FePO_4$ than in $LiFePO_4$.[26,27] However, a 1 V s^{-1} rate is likely to create a non negligible ohmic drop despite the addition of conducting carbon additive. As a result, any interpretation of the phenomenon occurring in this rate range must be done cautiously and further refinements are needed. Furthermore, the relative charge measured at 1 V s^{-1} gives 40% of the Q_0 value obtained at 0.1 mV s^{-1}. This high rate capability reflects the excellent Li$^+$ displacement into the LFP structure, and makes it relevant for the use in power devices.

Table I. k_1 and k_2 coefficients for the anodic and cathodic peaks of the CV curves.

	Zone 1		Zone 2-a		Zone 2-b	
	$k_1 (\mu A\ s\ V^{-1})$	$k_2 (\mu A\ s^{1/2}\ V^{-1/2})$	$k_1 (\mu A\ s\ V^{-1})$	$k_2 (\mu A\ s^{1/2}\ V^{-1/2})$	$k_1 (\mu A\ s\ V^{-1})$	$k_2 (\mu A\ s^{1/2}\ V^{-1/2})$
Anodic peak	8.86	0.97	0	1.53	0.09	1.43
Cathodic peak	–5.41	–0.88	–0.07	–1.24	–0.31	–1.16

The surprisingly good rate performance of LiFePO$_4$ has already been explained[14] as the lithiation/delithiation of the olivine takes place within a low-order boundary between the two Li-rich and Li-poor phases. This destabilized boundary is believed to be created by the crystallographic mismatch between those two phases, leading to a zone through which the Li$^+$ ions can easily diffuse in the b-axis, while the phase boundary is moving towards the a-axis. The high rate charging/discharging may also expand this interphase region through which the Li$^+$ ions move, and consequently increases the rate capability of the material.[8]

Conclusion

The extremely high charge/discharge rates applied to the LFP up to 1 V s^{-1} enabled by a cavity microelectrode allows focusing on the intrinsic kinetic properties of the material on a broad range of scan rate. It shows that the lithiation and delithiation processes are not diffusion-limited at low scan rate, where the reaction takes place within the entire bulk of the LFP. The system is controlled by the diffusion of the Li$^+$ ions from 5 mV s^{-1}. Despite the mass transport control of the electrochemical reaction, the LFP was able to sustain very high power regimes, since 40% of the Q_0 slow rate capacity was measured at 1 V s^{-1}. The high rate capability may be due to an increasing contribution of fast charge transfer in the active sites located at the surface of the particles, traduced by an increase of the k_1 coefficient.

Acknowledgments

References

1. A. K. Padhi, K. S. Nanjundaswamy, and J. B. Goodenough, *J. Electrochem. Soc.*, **144**, 1188 (1997).
2. A. K. Padhi, K. S. Nanjundaswamy, C. Masquelier, S. Okada, and J. B. Goodenough, *J. Electrochem. Soc.*, **144**, 1609 (1997).
3. N. Ravet, Y. Chouinard, J. F. Magnan, S. Besner, M. Gauthier, and M. Armand, *J. Power Sources*, **97**, 503 (2001).
4. A. V. Churikov, A. V. Ivanishchev, V. O. Sycheva, N. R. Khasanova, and E. V. Antipov, *Electrochim. Acta*, **55**, 2939 (2010).
5. X.-C. Tang, L.-X. Li, Q.-L. Lai, X.-W. Song, and L.-H. Jiang, *Electrochim. Acta*, **54**, 2329 (2009).
6. A. Yamada, S. C. Chung, and K. Hinokuma, *J. Electrochem. Soc.*, **148**, A224 (2001).
7. B. Kang and G. Ceder, *Nature*, **458**, 190 (2009).
8. G. Chen, X. Song, and T. J. Richardson, *Electrochem. Solid-State Lett.*, **9**, A295 (2006).
9. S.-I. Nishimura, G. Kobayashi, K. Ohoyama, R. Kanno, M. Yashima, and A. Yamada, *Nature Mater.*, **7**, 707 (2008).
10. W. Sigle, R. Amin, K. Weichert, P. A. Van Atken, and J. Maier, *Electrochem. Solid-State Lett.*, **12**, A151 (2009).
11. P. Gibot, M. Casas-Cabanas, L. Laffont, S. Levasseur, P. Carlach, S. Hamelet, J.-M. Tarascon, and C. Masquelier, *Nature Mater.*, **7**, 741 (2008).
12. J. L. Allen, T. R. Jow, and J. Wolfenstine, *Chem. Mater.*, **19**, 2108 (2007).
13. W. Dreyer, J. Jamnik, C. Guhlke, R. Huth, J. Moskon, and M. Gaberscek, *Nature Mater.*, **9**, 448 (2010).
14. C. Delmas, M. Maccario, L. Croguennec, F. Le Cras, and F. Weill, *Nature Mater.*, **7**, 665 (2008).
15. C. V. Ramana, A. Mauger, F. Gendron, C. M. Julien, and K. Zaghib, *J. Power Sources*, **187**, 555 (2009).
16. M. S. Islam, D. J. Driscoll, C. A. J. Fisher, and P. R. Slater, *Chem. Mater.*, **17**, 5085 (2005).
17. C. Delacourt, P. Poizot, S. Levasseur, and C. Masquelier, *Electrochem. Solid-State Lett.*, **9**, A352 (2006).
18. M. Okubo, E. Hosono, J. Kim, M. Enomoto, N. Kojima, T. Kudo, Ha. Zhou, and I. Honma, *J. Am. Chem. Soc.*, **129**, 7444 (2007).
19. D.Y. W. Yu, C. Fietzek, W. Weydanz, K. Donoue, T. Inoue, H. Kurokawa, and S. Fujinati, *J. Electrochem. Soc.*, **154**, A253 (2007).
20. H. Matsui, T. Nakamura, Y. Kobayashi, M. Tabuchi, and Y. Yamada, *J. Power Sources*, **195**, 6879 (2010).
21. S. Franger, C. Bourbon, and F. LeCras, *J. Electrochem. Soc.*, **151**, A1024 (2004).
22. F. Sauvage, E. Baudrin, M. Morcrette, and J.-M. Tarascon, *Electrochem. Solid-State Lett.*, **7**, A15 (2004).
23. C. Delacourt, L. Laffont, R. Bouchet, C. Wurm, J.-B. Leriche, M. Mocrette, J.-M. Tarascon, and C. Masquelier, *J. Electrochem. Soc.*, **152**, A913 (2004).
24. A. J. Bard and L. R. Faulkner, in *Electrochemical Methods: Fundamentals and Applications*, 2nd ed., p. 233, John Wiley & Sons, New York (2001).
25. J. Wang, J. Polleux, J. Lim, and B. Dunn, *J. Phys. Chem. C*, **111**, 14925 (2007).
26. T. Maxisch, F. Zhou, and G. Ceder, *Phys. Rev. B*, **73**, 104301 (2006).
27. V. Srinivasan and J. Newman, *Electrochem. Solid-State Lett.*, **9**, A110 (2006).